NASA Technical Memorandum 107089

Thermal and Structural Analysis of a Hollow Core Space Shuttle Main Engine (SSME) Turbine Blade

Ali Abdul-Aziz and Sreeramesh Kalluri
NYMA, Inc.
Brook Park, Ohio

Michael A. McGaw
Lewis Research Center
Cleveland, Ohio

December 1995

National Aeronautics and
Space Administration

THERMAL AND STRUCTURAL ANALYSIS OF A HOLLOW CORE SPACE SHUTTLE MAIN ENGINE (SSME) TURBINE BLADE

Ali Abdul-Aziz and Sreeramesh Kalluri
NYMA, Inc.
Brook Park, Ohio 44142

and

Michael A. McGaw*
National Aeronuatics and Space Administration
Lewis Research Center
Cleveland, Ohio 44135

SUMMARY

The influence of primary and secondary orientations on the elastic response of a hollow core, [001]-oriented nickel base single-crystal superalloy turbine blade, was investigated under combined thermal and mechanical loading conditions. Finite element technique is employed through MARC finite element code to conduct the analyses on a hollow core SSME turbine blade made out of PWA 480 single crystal material. Primary orientation of the single crystal superalloy was varied in increments of 2°, from 0 to 10°, from the [001] direction. Two secondary orientations (0 and 45°) were considered, with respect to the global coordinate system, as the primary orientation angle was varied. The stresses developed within the single crystal blade were determined for different orientations of the blade. The influence of angular offsets such as the single crystal's primary and secondary orientations and the loading conditions on the elastic stress response of the PWA 1480 hollow blade are summarized. The influence of the primary orientation angle, when constrained between the bounds considered, was not found to be as significant as the influence of the secondary orientation angle.

INTRODUCTION

Hot section components of spacecraft engines are exposed to severe thermal-structural loading conditions, especially during the start-up and shutdown portions of the engine cycle. For instance, the thermal transient during start-up conditions within the Space Shuttle Main Engine (SSME) could lead to a gas temperature in excess of 3000 °C which causes high stresses and strains that affect the operating life of key components such as the turbine blades. These extreme conditions are generally driven by the steep thermal gradients during ignition and main stage operating periods.

To improve the durability of these components and in particular the turbine blades, a new generation of materials have been considered. Among these materials are the single crystal (SC) superalloys. They were cited to be the materials of choice to develop a new generation of turbopump blades for the SSME and other advanced rocket engines (refs. 1 and 2). The first engine company to take the lead in considering the single crystals as a blade

*Presently with McGaw Technology, Inc., P.O. Box 26268, Fairview Park, Ohio 44126.

materials was Pratt & Whitney Aircraft Company. They have selected a nickel-base single crystal superalloy, PWA 1480, as the material to be used in the fabrication of blades for the Alternate Turbopump Development (ATD) program for the SSME.

Turbine blades made out of single crystal superalloys including PWA 1480 are directionally solidified along the low modulus [001] crystallographic direction. It is known that this arrangement will enhance thermal fatigue resistance (ref. 1). The directional solidification process usually generates a secondary crystallographic direction, [010] that is randomly oriented with respect to fixed geometric axes in the turbine blade. However, control of the secondary orientation of the crystallographic direction is possible by using a seed crystal during the solidification process (ref. 3). Moreover, due to the anisotropic nature of the single crystal, the stress-strain response and the dynamic characteristics of any component made out of single crystal, such as the turbine blades, would depend on both the primary and the secondary orientations angles (refs. 4 and 5). Investigation by Kalluri et al. (ref. 6), and Abdul-Aziz et al. (ref. 7) showed that the influence of the primary orientation was not as significant as the secondary orientation. This was established after investigating the stresses developed in a SC PWA 1480 square plate that was subjected to both mechanical and thermal loads.

The purpose of this work is to investigate the crystal orientation effects further by analyzing a structure with specified operating conditions such as the SSME turbine blade. The main difference between the current work and previous investigations (refs. 6 and 7) is that the present analyses are conducted under actual operating conditions as compared to those used in the simulated square plate investigation. The current study is intended to further substantiate the findings reported in references 6 and 7.

Therefore, an elastic analysis is conducted to evaluate the structural response of a [001]-oriented, hollow-core, SC PWA 1480 SSME turbine blade subjected to thermal, mechanical and combined thermal and mechanical loads. The primary orientation [001] was varied in increments of 2° from 0 to 10° with respect to a global coordinate system for two sets of secondary orientation angles of 0 and 45°. These two secondary orientations were found to represent two extremes cases (ref. 6).

PROBLEM DESCRIPTION

The first stage high pressure fuel turbopump turbine blade of the SSME was selected for this study because of its history of early crack initiation and other durability problems. This is a hollow blade and is made of SC PWA 1480, with the span of the blade along [001] crystallographic direction (primary orientation) and a maximum allowable angular deviation of no greater than 10°.

In this design, the hollow core extends below the platform into the shank region, see figures 1 and 2. The XYZ-axes shown in Figure 3 represent the global coordinate system, with the Z-axis along the span, Y-axis along the chord and the X-axis along the thickness of the blade.

The SSME turbine blades are typically subjected to severe loading conditions during normal operations. These loads usually consist of a combination of centrifugal, steady and oscillatory forces as well as thermal loading due to the steep thermal gradients. The blades are generally cooled except for their airfoils which are exposed to hot gas flow path that produces high thermal gradients both along the span and through the thickness. The thermal gradient through the thickness is on the order of 875 °C/cm (ref. 8), which is much higher than the gradient along the span of the blade, figure 4. To-date the thermal environment conditions at the platform and shank regions are not well defined due to the complexity of cooling gas flow and the blade geometry.

ANALYTICAL PROCEDURE

Elastic stress analyses were conducted on the hollow core blade shown in figure 1 by using the MARC finite element code (ref. 9). The blade consists of four sections: airfoil, platform, shank and firtree. The hollow

airfoil has a span length of 2.2 cm and a span-to-chord width aspect ratio of approximately unity. It is highly cambered and the cross-section is nearly constant along the slightly twisted blade span and its four-lobed firtree section mates with the rotor. The firtree attachments were excluded from the analyses due to lack of information regarding their thermal environment. The firtree effects were simulated by boundary conditions applied to the shank region.

The present blade geometry is illustrated in figure 1. A finite element model of the hollow core blade was developed using the typical geometry of the SSME solid blade of the first stage high pressure fuel turbo-pump (ref. 10). A hollow section was introduced within the solid blade that extended beneath the platform into the shank region. Limited knowledge and unavailability of the hollow blade geometric dimensions led to the use of the solid blade geometry to generate the hollow core finite element model. The three dimensional finite element model consisting of 959 eight-node isoparametric brick elements and 1575 nodes is shown in figure 5.

The two coordinate systems are shown in figure 3, the XYZ being the global coordinate system and the $X_cY_cZ_c$ being the crystal coordinate system. For example, the transformation for any secondary orientation is obtained by rotat-ing the crystal coordinate system about the Z_c-axis by an angle of θ. Since the Z and Z_c are both oriented along the [001] crystallographic direction, the angle θ between the crystal and the global coordinate systems represents the orientation of secondary crystallographic direction. The matrix of direction cosines that relates the global coordinate system to the crystal coordinate system (fig. 3) is as follows:

$$\begin{pmatrix} x \\ y \\ z \end{pmatrix} = \begin{bmatrix} \cos\theta & \sin\theta & 0 \\ -\sin\theta & \cos\theta & 0 \\ 0 & 0 & 1 \end{bmatrix} \begin{pmatrix} x_c \\ y_c \\ z_c \end{pmatrix} \tag{1}$$

Details regarding the implementation of the stiffness coefficient matrices in the finite element code as well as the method applied to derive the elastic stiffness coefficients of a single crystal in the global coordinate system are exclusively explained in references 6 and 7.

A. Heat Transfer Analysis

The thermal environment experienced by the hollow core blade is not readily available. As an approximation to predict the blade temperature, data from the thermal environment of solid blade were used [8]. This approximation is deemed acceptable due to the similarities in the fluid flow conditions surrounding external configuration of both blades.

In conducting the heat transfer analysis, assumptions were made to simplify the problem and at the same time to preserve accuracy. These assumptions were as follows: (1) the variations of the hot-gas temperature profiles in the radial and circumferential directions were assumed negligible, (2) the blade tip and shank base were assumed to be insulated, (3) the internal hollow core section was assumed insulated for the airfoil region only, and (4) steady state conditions were considered for the entire analysis.

The thermal boundary conditions for the platform-shank region covered several phenomena of heat transfer. They were incorporated in the thermal model through MARC user's subroutine feature. The heat transfer phenomena experienced are: (1) conduction through the thickness, (2) convection between the blade surface and the flow of a mixture of hot-cold gases on the outer region as well as convection along the surface of the hollow core section. The conduction was implemented by estimating the thermal gradient experienced through the thickness using the experimental data (ref. 8) and by using the gas temperature and film coefficients from reference 10. This covered the entire outer region of the blade including the platform and the shank areas. The gas temperature during steady state conditions was estimated to be about 785 °C near the airfoil, 679 °C near the platform and 479 °C near the shank section (ref. 11).

B. Stress Analysis

The thermal-structural elastic finite element analysis was initiated after a completed thermal analysis including a well defined temperature. The variation of the stiffness matrix for various primary orientations ($\psi = 0°$ to $10°$ in increments of $2°$) and for the selected secondary orientations ($\theta = 0°$ and $45°$) were all incorporated in the MARC finite element calculations. The analyses included accounting for temperature dependencies of all the physical properties used. Temperature dependent material properties required to describe the elastic behavior of a cubic single crystal such as the SC PWA 1480 within the crystallographic coordinate system were obtained from reference 6.

The stress analysis model consisted of 1575 nodes and 4667 unsuppressed degrees of freedom. Boundary conditions were applied by constraining all the nodes at the base of the shank to lie on a disk plane. Additional boundary conditions were imposed to prevent rigid body motion in the plane. Figure 2 shows the physical shape of the blade including all the attachments where the actual contact with the disk rotor is activated.

In addition to the thermal effects, the mechanical load considered in the analysis included the gas pressures and the centrifugal forces produced by the blade rotational speed (37 000 rpm) during steady state conditions. These data were supplied into the MARC code and analyses were conducted for the combined thermal and mechanical loads.

RESULTS AND DISCUSSION

The influence of both the primary and secondary orientation angles on the elastic response of a hollow core SC PWA 1480 blade under thermal and mechanical loading conditions are presented.

Contour plots of the temperature and stress fields of the blade are shown in figures 6 to 8. The airfoil temperatures are nearly independent of the conditions below the platform. However, the contour plot exhibits some variation in temperature across the span at the surface and the airfoil leading edge endures the highest temperature compared with the rest of the blade. The platform-shank junction shows a wide range of temperature variations, however, lack of knowledge of the thermal environment below the platform limits evaluation of this potential low-cycle fatigue driver. Further more having a coarse finite element mesh (i.e. only one element through the thickness) limited the evaluation of the effect of the through thickness thermal gradient on the stress response.

Figures 7 and 8 show the contour plots for the stress distributions on the blade. These contour plots were generated at steady state conditions and under combined effects of both thermal and mechanical loads. The stresses along the Z-axis or the [001] orientation are shown in figure 7 for both sides of the blade, (i.e. pressure and suction). The suction side of the blade experiences a nonuniform stress distribution with an apparent stress gradient at the junction of airfoil/platform region and a sizable stress concentration at the center of the shank near the base. This is an indication of the effects of the combined thermal and mechanical loads. The stress distribution on the pressure side is relatively uniform with the exception of some critical hot areas due to the temperature gradient at the airfoil-platform junction region. Figure 8 represents the distribution of the Von Mises stress on the suction side of the blade. The Von Mises stresses are highest at the center of the shank near the base and at the center of the airfoil near the platform. While the stress concentration at the airfoil is mainly due to thermal load effects the stress concentration at the shank is primary due to the centrifugal load caused by the high rotational speed and mechanical constraints.

The evaluation of the results led to the selection of four critical locations where failure initiation might occurs due to the presence of high stresses. Figure 5, shows these critical locations and they are labeled as elements 305 (at the airfoil base near the leading edge), 430 (shank leading edge below the platform), 444 (shank trailing edge below the platform) and 615 (shank base at center section). In addition to the analyses, hardware evidence showed that these locations on the blade experienced cracking and other durability problems (ref. 12).

The effects of the primary and secondary orientations on the stress responses of the critical locations are summarized in figures 9 to 12. Figures 9(a) and (b) show variations in the stress components under combined thermal and mechanical loading conditions for secondary orientation $\theta = 0^\circ$ and $\theta = 45^\circ$ as the primary orientation, ψ changed from 0 to 10° for element 305. As expected, the secondary orientation of 45° showed higher stresses. However, for this particular element the difference between the 0 and 45° is small. While for elements 430 and 444, (figs. 10 and 11), the effect of secondary orientation is significant. These locations are below the platform at the shank leading and trailing edges near the extended hollow cavity. The reason for these notable effects are due to the severe combined effects of the thermal gradient and the centrifugal load. The heat transfer through the cavity wall due to the hot gas on the inside versus the cold hydrogen flowing on the outside is the primary cause for this thermal gradient.

The influence of crystal orientation in the presence of complex loading situations is shown in the stresses of elements 430 and 444. For element 430, while σ_{yy} increased by 24 percent and σ_{zz} increased by 18 percent as the secondary orientation changed from 0° to 45°, variations in the stress components due to changes in the primary orientation are small. Similarly for element 444, a 33 percent increase is noted for σ_{yy} and about 20 percent is reported for σ_{xx}. In general, the shear stress components also exhibited small variations with the change in primary orientation. Figures 12(a) and (b) for element 615 show the variation of the stress components for mainly the mechanical loading. The stress levels as the secondary orientation varied from 0 to 45° have showed some differences. However, the maximum change in the stress levels for all components, is about 6 percent. For elements 430 and 444, the stresses have differed greatly because of the operating conditions in those regions. This leads to the conclusion that the effect of crystal orientation on the stresses generated under predominantly mechanical loading is minimal while under combined thermal and mechanical loading it is substantial. Finally, it must be noted, that the present analysis is only an elastic stress analysis, which limits the applicability of these findings.

CONCLUSIONS

An elastic finite element analysis under combined thermal and mechanical loading conditions was performed to determine the influence of the primary crystal orientation angle, for two different secondary orientation angles 0° and 45°, on [001]-oriented nickel-base single crystal superalloy (PWA 1480), hollow-core Space Shuttle Main Engine Turbine Blade. The primary orientation was varied from 0 to 10° in increments of 2° and the stresses developed within the turbine blade were computed. The following conclusions were drawn:

1. The results showed that the influence of the secondary orientation on the elastic stress response is very substantial. Highest stresses were developed at 45° secondary orientation.
2. The influence of the primary orientation angle, when constrained between 0 and 10°, on the elastic stresses generated within the turbine blade is much lower than the influence of the secondary orientation angle, which is not usually controlled.
3. This investigation on an SSME turbine blade has confirmed previous findings obtained from the analysis of a square plate.
4. This work is expected to offer an excellent base line for further studies on crystal orientation effects under inelastic conditions for advanced propulsion system components.

REFERENCES

1. Dreshfield, R.L., and Parr, R.A., "Application of Single Crystal Superalloys for Earth-To-Orbit Propulsion Systems," AIAA Paper 87-1976, 1987.
2. Fritzemeir, L.G., "Advanced Single Crystal for SSME Turbopumps," RI/RD 88-273, Rockwell International Corp., NASA CR-182244, 1989, pp. 1-44.
3. Duhl, D.N., "Single Crystal Superalloys," Superalloys, Supercomposites and Superceramics, J.K. Tien and T. Caulified, eds., Academic Press, Inc., 1989, pp. 149-182.
4. Bowen, K., Nagy, P., and Parr, R. A., "The Evaluation of Single Crystal Superalloys for the Turbopump Blades in the SSME," AIAA Paper 86-1477, 1986.
5. Abdul-Aziz, A., R. August and V. Nagpal, "Design Considerations for Space Shuttle Main Engine (SSME) Turbine Blade Made of Single Crystal Material, " Computer & Structures, Vol. 46, No. 2, pp. 249-259, January 1993.
6. Kalluri, S., Abdul-Aziz, A. and McGaw, M.A., " Elastic Response of [001]-Oriented PWA 1480 Single Crystal--The Influence of Secondary Orientation", SAE 1991 Transactions, Vol. 100, Journal of Aerospace, (section 1, part 1), pp. 273-283, September 1992.
7. Abdul-Aziz, A., Kalluri, S. and McGaw, M.A., "The Influence of Primary and Secondary Orientations on the Elastic Response of a Nickel-Base Single-Crystal Superalloy", ASME paper 93-GT-376, Presented at the 38th ASME International Gas Turbine and Aeroengine Congress and Exposition, May 24-27, 1993, Cincinnati, Ohio.
8. Lee, H. and Deniston, C., "Private Communication", NASA Marshall Space and Flight Center, 1992.
9. MARC General Purpose Finite Element Analysis Program, Vol. A: User Information manual; Vol. B: MARC Element Library; Vol. F: Theoretical Manual. MARC Analysis Corp., Palo Alto, CA, 1988.
10. Abdul-Aziz, A., Tong, T.M and Kaufman, A.,"Thermal Finite-Element Analysis of Space Shuttle Main Engine Turbine Blade," Finite Elements in Analysis and Design, Vol. 5, pp. 337-348, November 1989.
11. Depsky, J., "Private Communication", Rockwell International, Rocketdyne Division, 1988.
12. Turbine Blade Analysis Team, "SSME Turbine Blade Analysis Team Report", Rockwell International, Rocketdyne division, RSS-8732, Contract NASA-27980, December, 10, 1986.

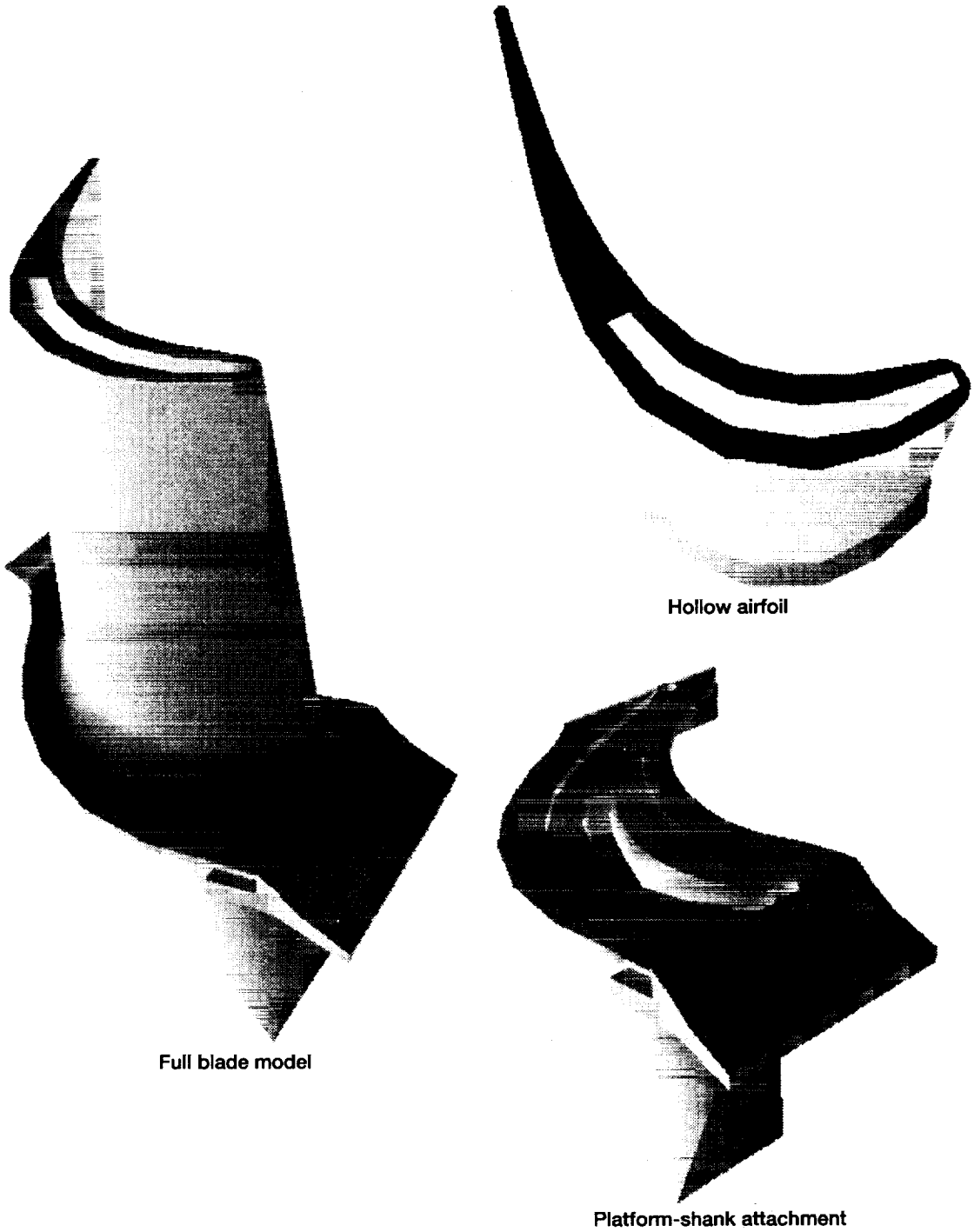

Figure 1.—High pressure fuel turbopump's first stage hollow core blade geometry.

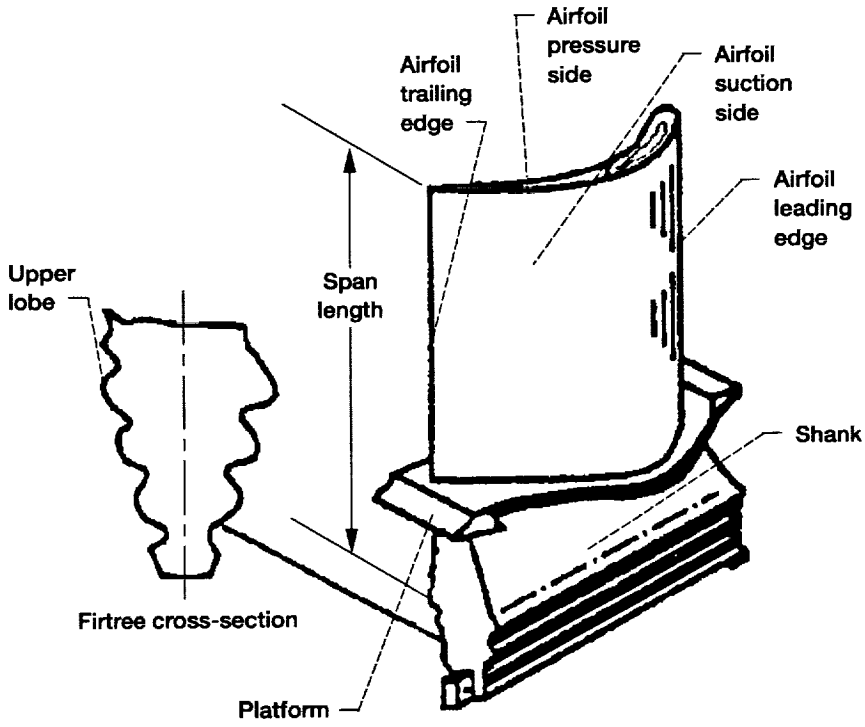

Figure 2.—First stage turbine blade of high pressure fuel turbopump (HPFTP).

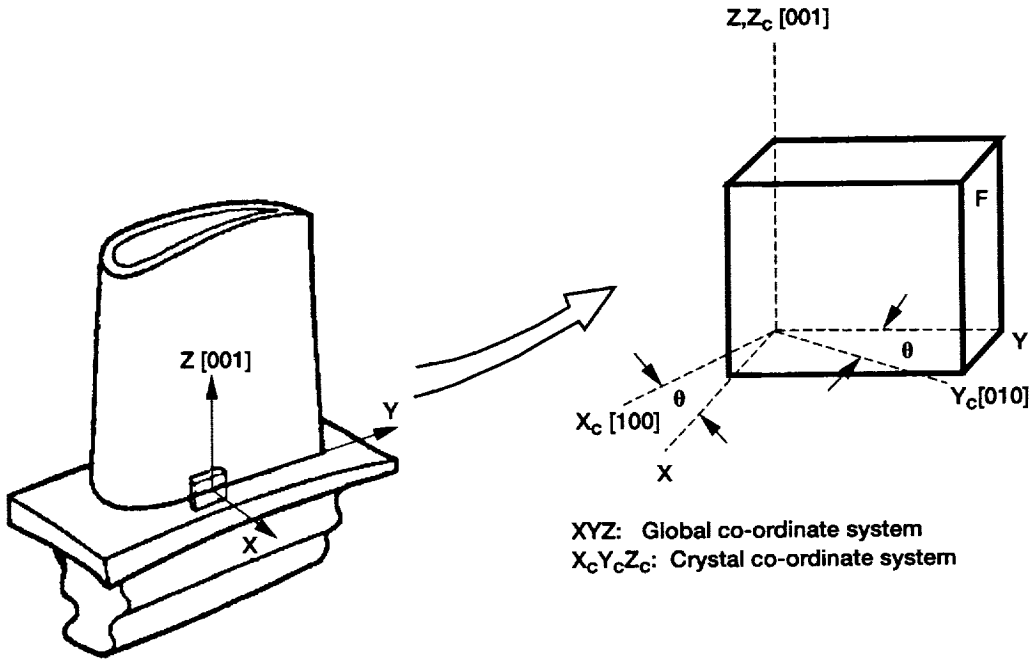

Figure 3.—Schematics of the hollow-core turbine blade and an element in the blade.

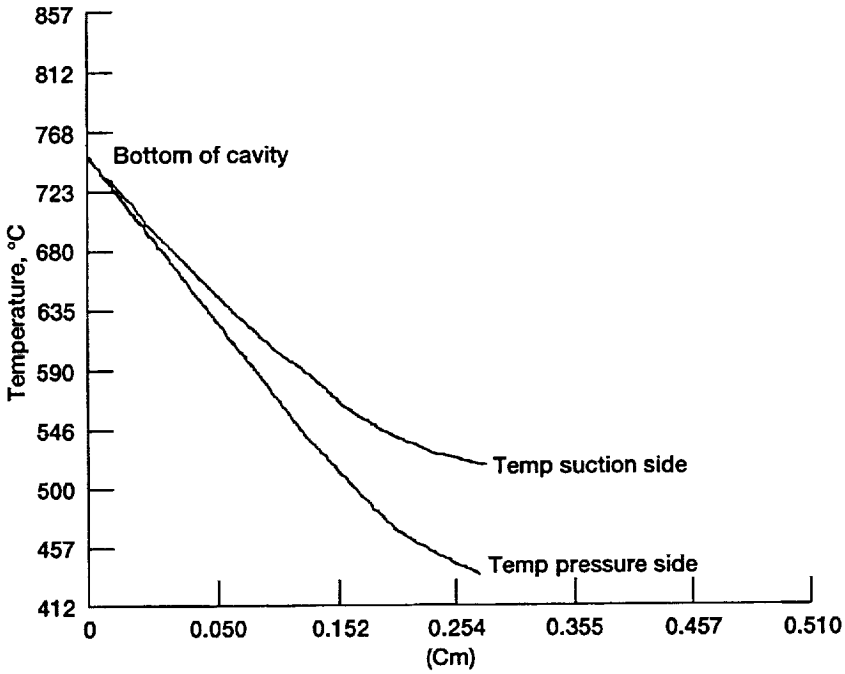

Figure 4.—Temperature profile through the blade's plarform-shank region [8].

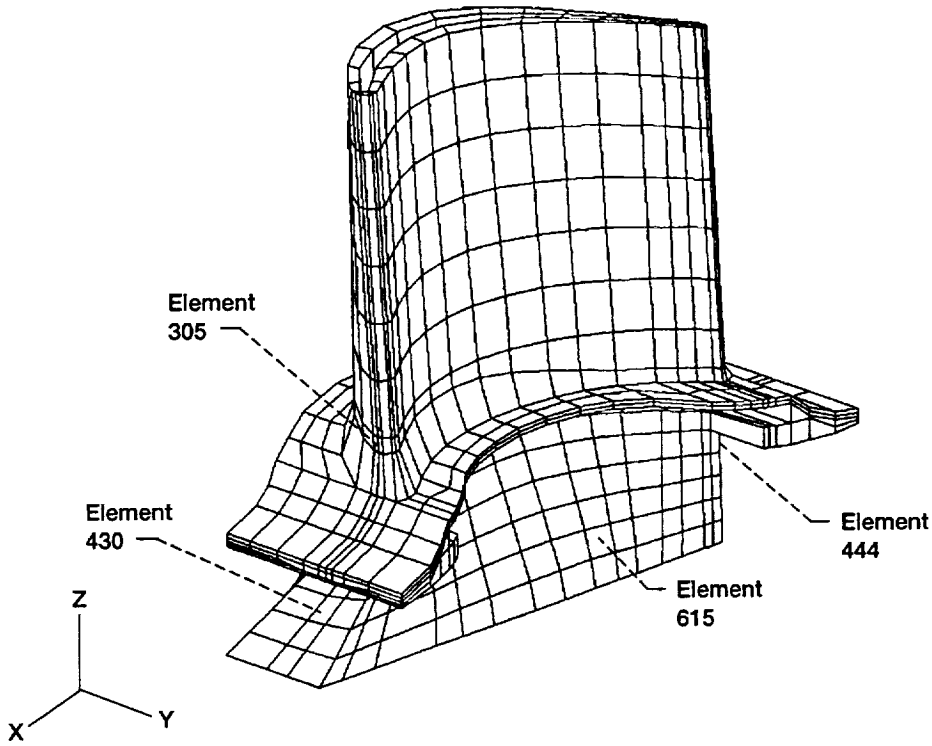

Figure 5.—Finite element model of the hollow-core blade.

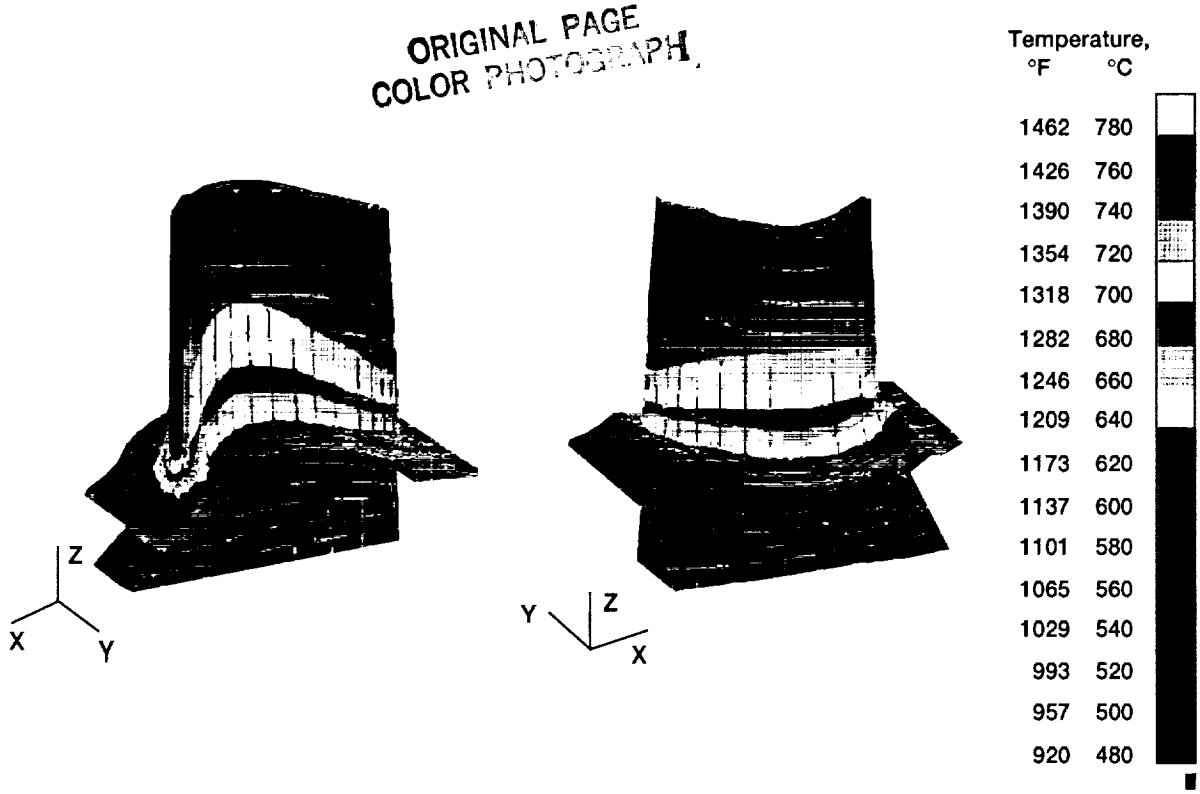

Figure 6.—Steady state temperature distribution.

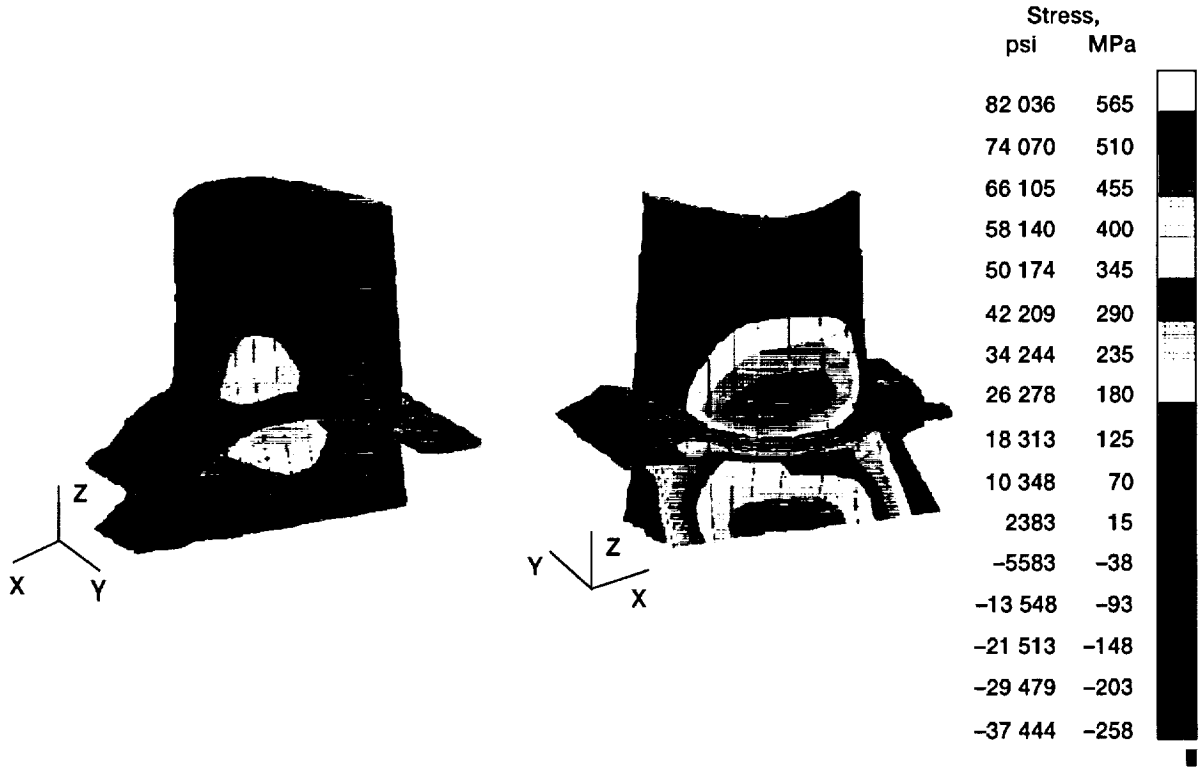

Figure 7.—Stresses along the Z-direction for secondary orientation of 45° under combined loading conditions.

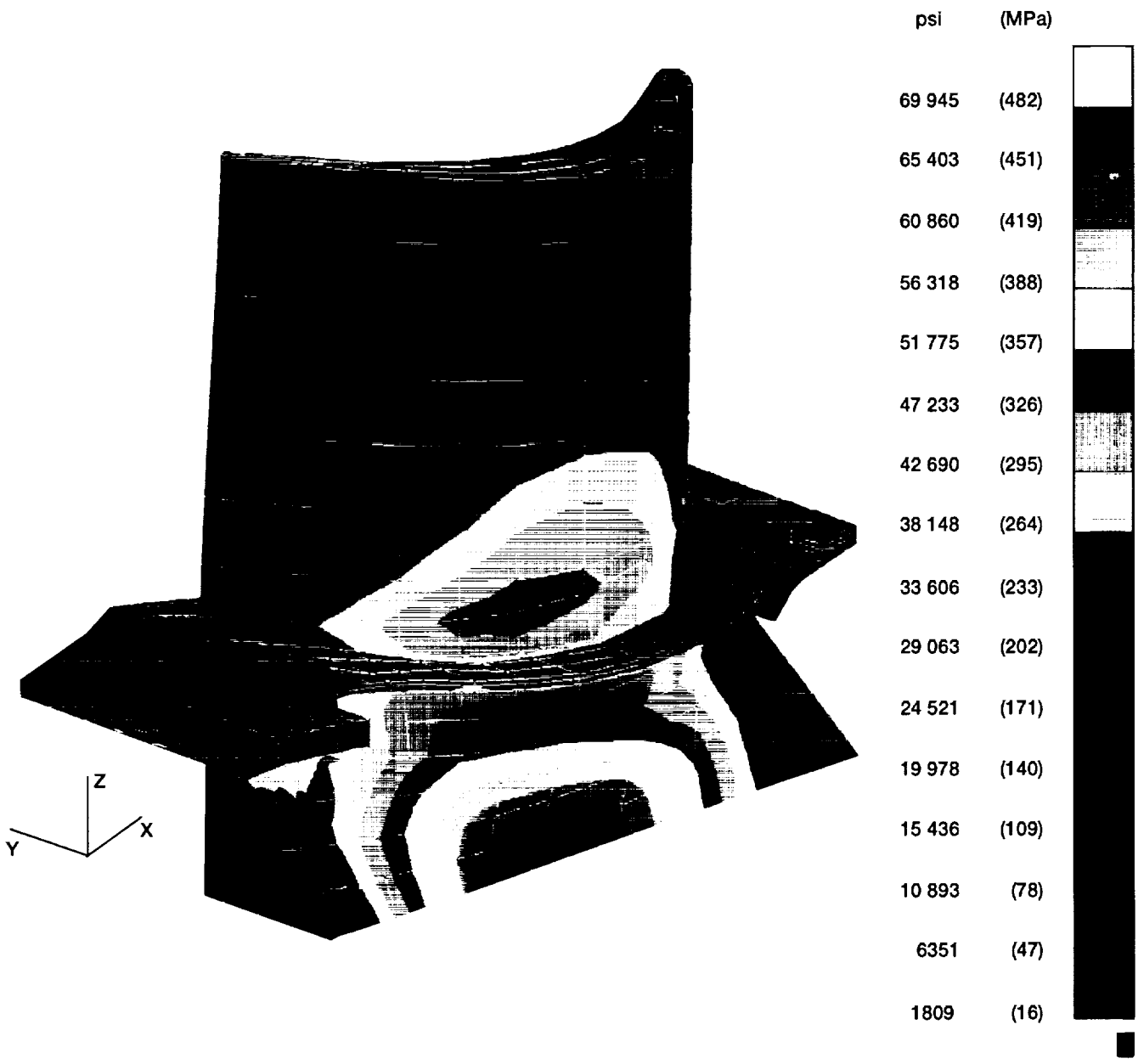

Figure 8.—Von mises stresses for secondary orientation of 45° under combined loading conditions.

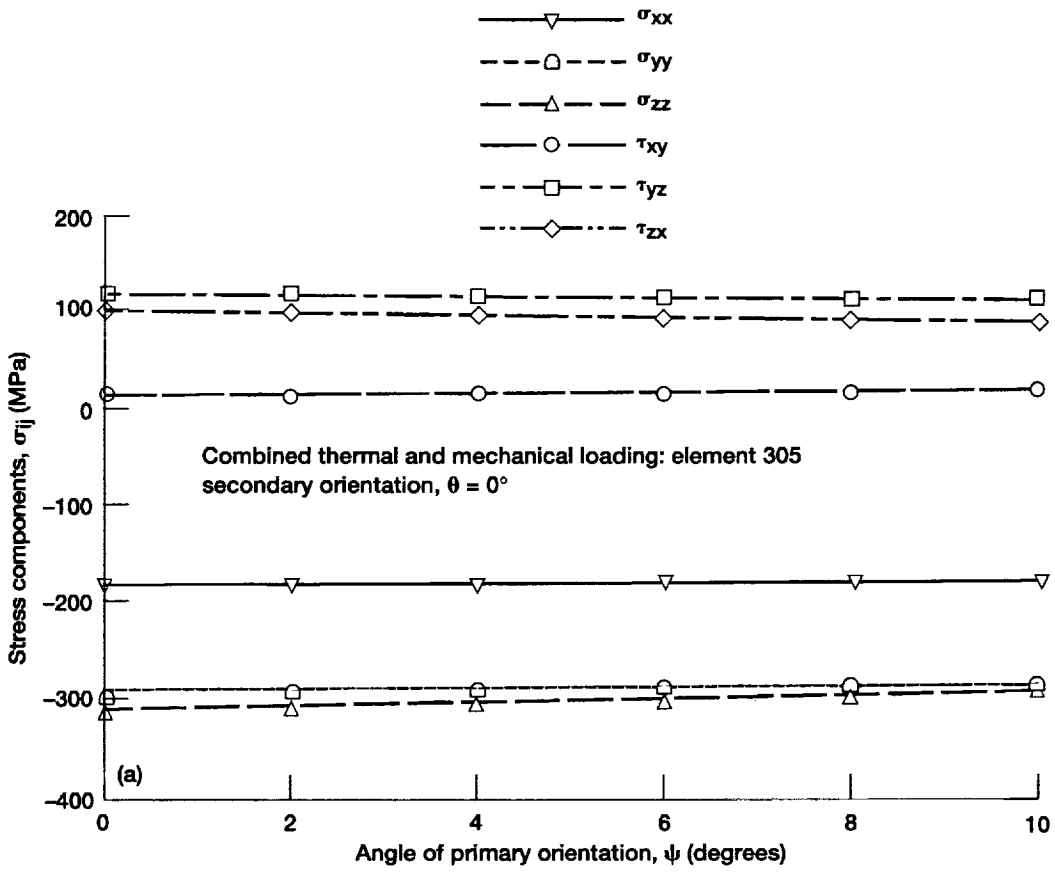

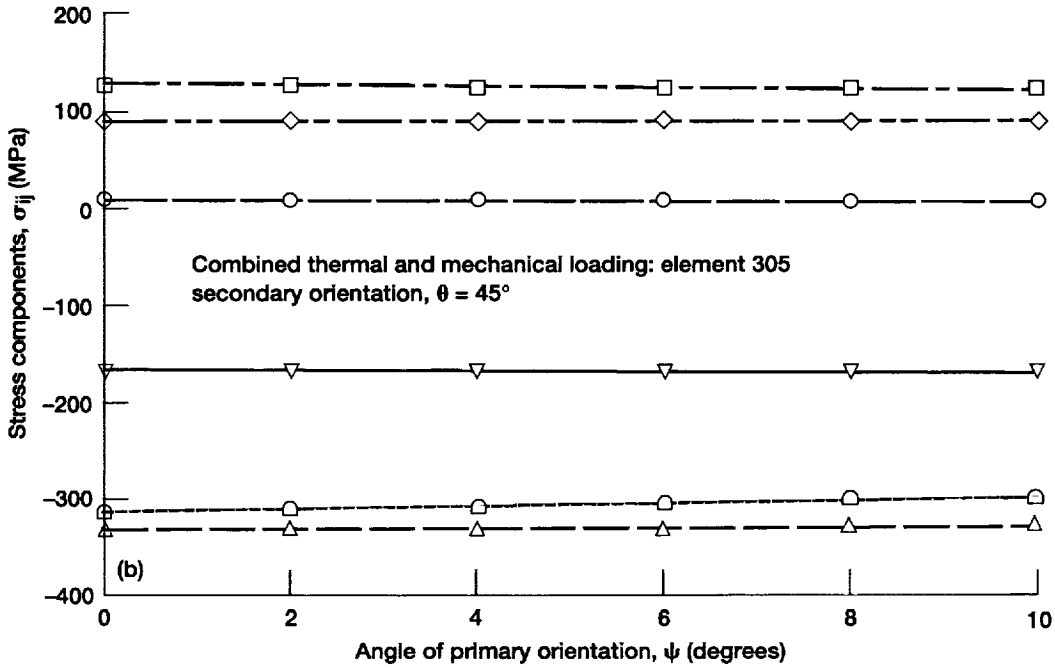

Figure 9.—(a) Influence of secondary orientation, 0°, and primary orientations under combined thermal and mechanical loads for element 305. (b) Influence of secondary orientation, 45°, and primary orientations under combined thermal and mechanical loads for element 305.

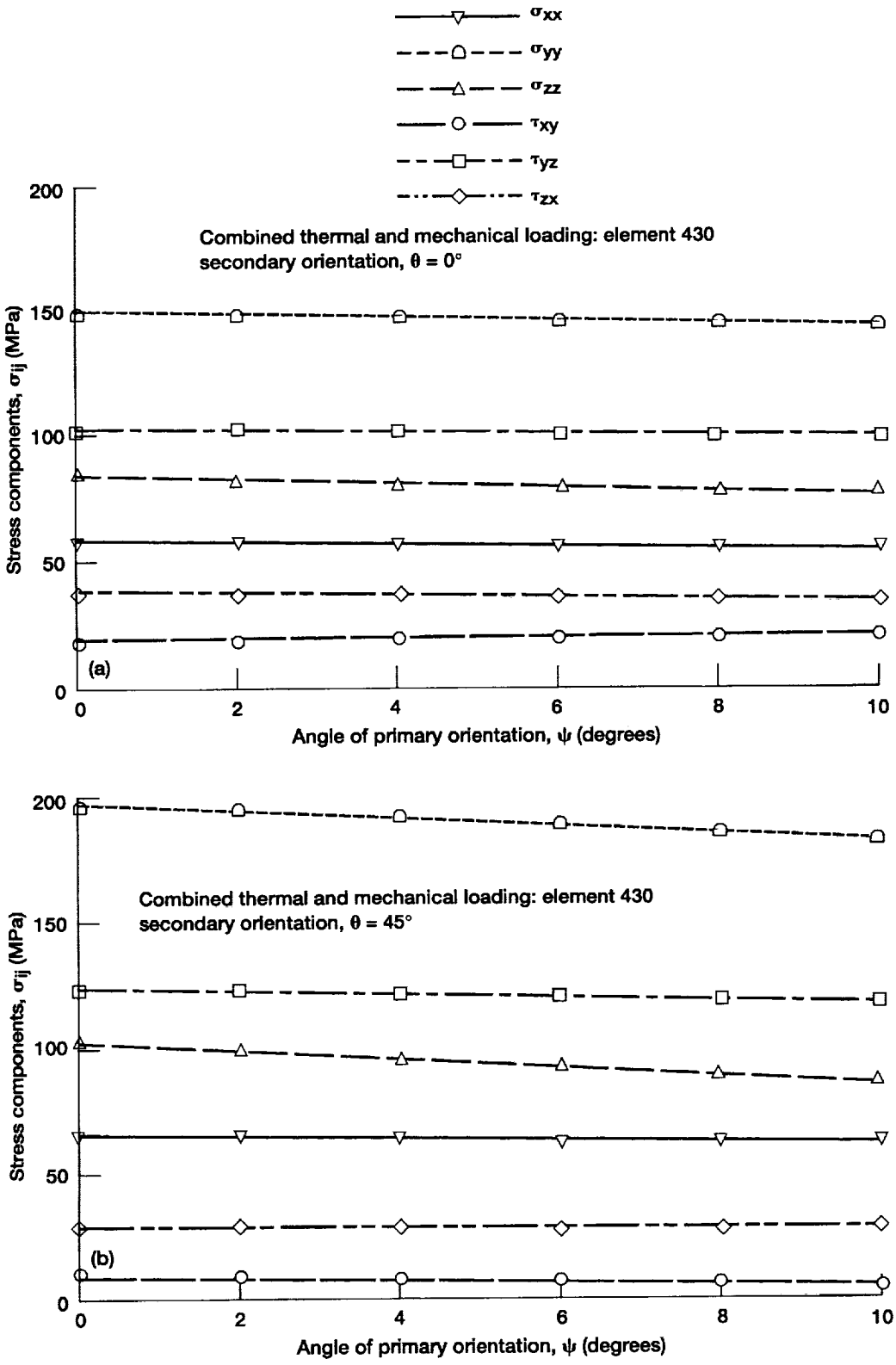

Figure 10.—(a) Influence of secondary orientation, 0°, and primary orientations under combined thermal and mechanical loads for element 430. (b) Influence of secondary orientation, 45°, and primary orientations under combined thermal and mechanical loads for element 430.

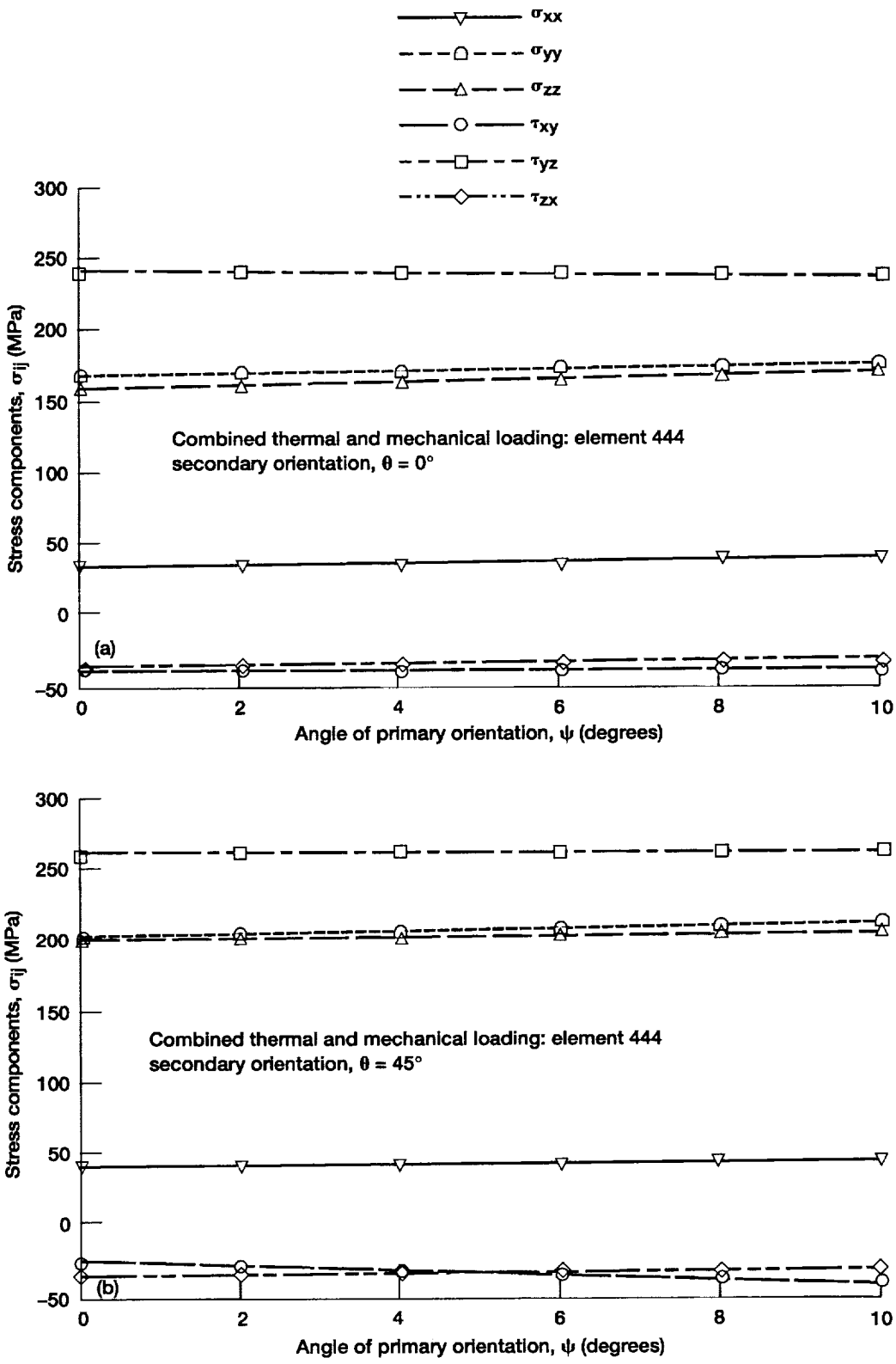

Figure 11.—(a) Influence of secondary orientation, 0°, and primary orientations under combined thermal and mechanical loads for element 444. (b) Influence of secondary orientation, 45°, and primary orientations under combined thermal and mechanical loads for element 444.

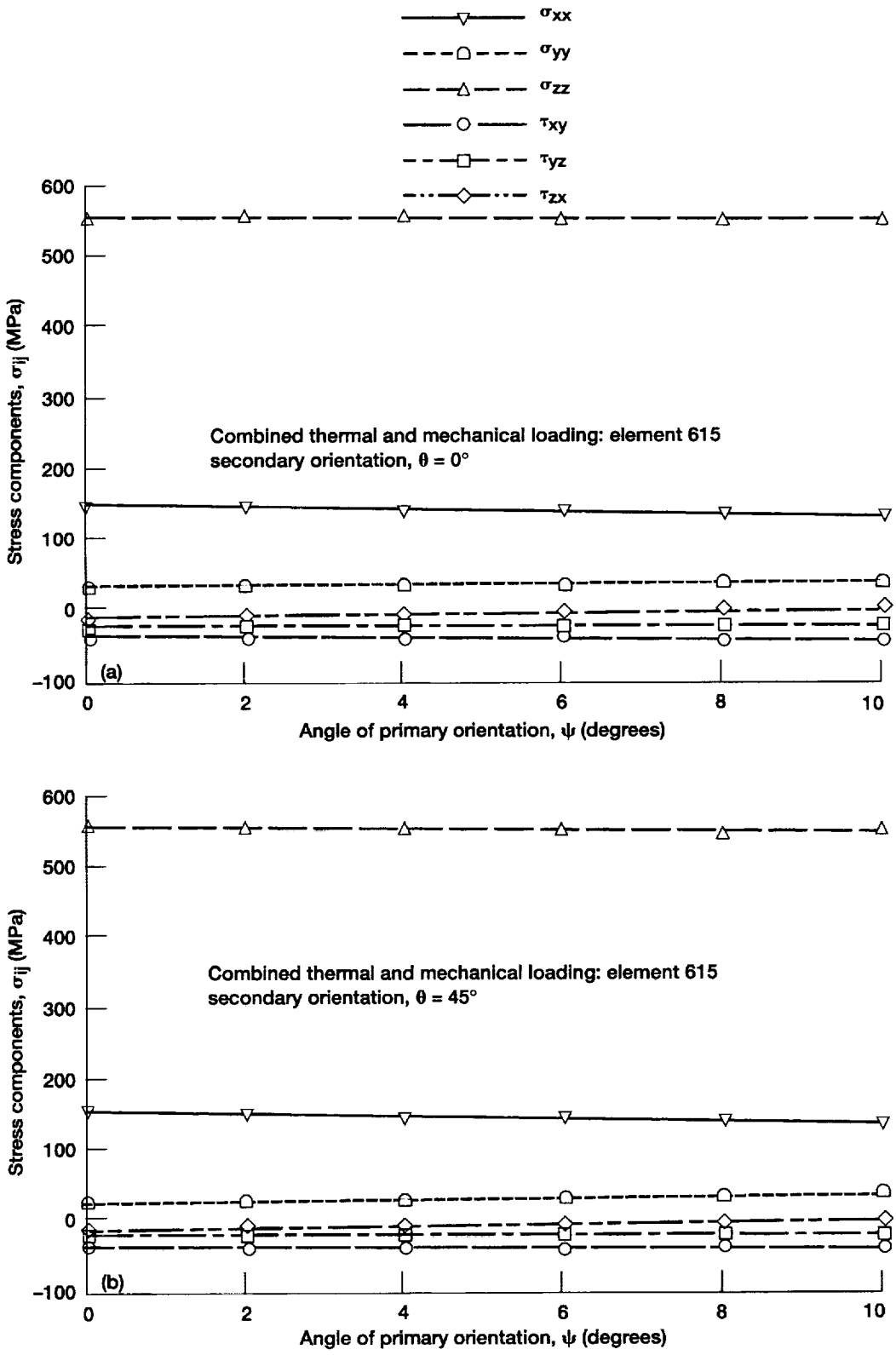

Figure 12.—(a) Influence of secondary orientation, 0°, and primary orientations under combined thermal and mechanical loads for element 615. (b) Influence of secondary orientation, 45°, and primary orientations under combined thermal and mechanical loads for element 615.

REPORT DOCUMENTATION PAGE

Form Approved
OMB No. 0704-0188

1. AGENCY USE ONLY (*Leave blank*)	2. REPORT DATE	3. REPORT TYPE AND DATES COVERED
	December 1995	Technical Memorandum

4. TITLE AND SUBTITLE

Thermal and Structural Analysis of a Hollow Core Space Shuttle Main Engine (SSME) Turbine Blade

5. FUNDING NUMBERS

WU-505-63-5B

6. AUTHOR(S)

Ali Abdul-Aziz, Sreeramesh Kalluri, and Michael A. McGaw

7. PERFORMING ORGANIZATION NAME(S) AND ADDRESS(ES)

National Aeronautics and Space Administration
Lewis Research Center
Cleveland, Ohio 44135-3191

8. PERFORMING ORGANIZATION REPORT NUMBER

E-9967

9. SPONSORING/MONITORING AGENCY NAME(S) AND ADDRESS(ES)

National Aeronautics and Space Administration
Washington, D.C. 20546-0001

10. SPONSORING/MONITORING AGENCY REPORT NUMBER

NASA TM-107089

11. SUPPLEMENTARY NOTES

Ali Abdul-Aziz and Sreeramesh Kalluri, NYMA, Inc., 2001 Aerospace Parkway, Brook Park, Ohio 44142 (work performed under NASA Contract NAS3-27186), and Michael A. McGaw, NASA Lewis Research Center, presently with McGaw Technology, Inc., P.O. Box 26268, Fairview Park, Ohio 44126. Responsible person, Rod Ellis, organization code 5220, (216) 433-3340.

12a. DISTRIBUTION/AVAILABILITY STATEMENT

Unclassified - Unlimited
Subject Category 39

This publication is available from the NASA Center for Aerospace Information, (301) 621-0390.

12b. DISTRIBUTION CODE

13. ABSTRACT (*Maximum 200 words*)

The influence of primary and secondary orientations on the elastic response of a hollow core, [001]-oriented nickel base single-crystal superalloy turbine blade, was investigated under combined thermal and mechanical loading conditions. Finite element technique is employed through MARC finite element code to conduct the analyses on a hollow core SSME turbine blade made out of PWA 1480 single crystal material. Primary orientation of the single crystal superalloy was varied in increments of 2°, from 0 to 10°, from the [001] direction. Two secondary orientations (0 and 45°) were considered, with respect to the global coordinate system, as the primary orientation angle was varied. The stresses developed within the single crystal blade were determined for different orientations of the blade. The influence of angular offsets such as the single crystal's primary and secondary orientations and the loading conditions on the elastic stress response of the PWA 1480 hollow blade are summarized. The influence of the primary orientation angle, when constrained between the bounds considered, was not found to be as significant as the influence of the secondary orientation angle.

14. SUBJECT TERMS

Structural analysis; Single crystal; Primary and secondary orientation; SSME blade

15. NUMBER OF PAGES

20

16. PRICE CODE

A03

17. SECURITY CLASSIFICATION OF REPORT	18. SECURITY CLASSIFICATION OF THIS PAGE	19. SECURITY CLASSIFICATION OF ABSTRACT	20. LIMITATION OF ABSTRACT
Unclassified	Unclassified	Unclassified	